

Electrorheology of undoped poly(*p*-phenylene) particle-based suspension

J.-I. SOHN

Department of Chemistry, Hallym University, Chunchon, 200-702, Korea
E-mail: jisohn@hallym.ac.kr

J. H. SUNG, H. J. CHOI

Department of Polymer Science and Engineering, Inha University, Incheon, 402-751, Korea

M. S. JHON

Department of Chemical Engineering, Carnegie Mellon University, Pittsburgh, PA 15213-3890, USA

Electrorheological (ER) properties of synthesized, pristine poly(*p*-phenylene) (PPP) particles without any dopant treatment was investigated via flow curves including shear viscosity and yield stress. The ER characteristics were examined as functions of both particle concentration and applied electric field strengths. This undoped, PPP based suspension exhibited normal ER characteristics displayed by conventional semi-conducting polymeric ER materials with doping. The yield stress, which is an important design parameter for ER fluids, satisfied a universal scaling function. We found that the critical electric field strength for the undoped PPP suspension was much higher than the doped PPP suspension. These undoped particles can be used as a model system to test the doped system at low concentration via a universal scaling function. © 2002 Kluwer Academic Publishers

1. Introduction

Electrorheological (ER) fluids are a class of materials whose rheological properties including yield stress and shear viscosity are controllable by tuning the imposed external electric field strength. Typical ER response shows a rapid and reversible change in suspension viscosity under an electric field, which also results in substantial changes in the suspension micro structure from an initial random distribution of particles to a more ordered fibrillated structure which span the electrode gap [1, 2]. Qualitatively, the ER particles are polarized by the external electric field and the interaction among the resulting dipoles cause the particles to form fibrillated structures aligned with the electric field direction, and produce ER response. The reorientation of dispersed particles whose initial random distribution transforms into fibrillated structure result in the change of shear viscosity to a higher value [3]. Note that, all of the physical and mechanical properties of the ER fluids induced by the applied electric field are reversible [4, 5].

A wide variety of particulate materials have been selected to prepare ER suspensions. They are: starch, flour, silica, alumina, titania, zeolite, and semi-conducting polymers. Among these, semi-conducting polymer based ER fluids are commonly used as ER systems. The anhydrous ER materials including polyaniline [6, 7], copolystyrene particles coated with polyaniline [8], poly(aniline-co-*o*-ethoxyaniline) [9], poly(acenequinone) radicals [10], and poly(*p*-phenylene)

(PPP) [11], are polarizable and conductive material. The intra- and intermolecular-structure of conducting polymers and the associated structural behavior are fundamental properties which strongly impact the physical properties manifested by this unique class of materials. Even relatively small changes in a specific chemical architecture and processing condition can lead to significant variations in the resultant structures and their physical properties. The homogeneous solutions of liquid crystals are sometimes added to improve colloidal stability of the dispersed particles as well as to enhance ER activity [12–14]. Besides the semi-conducting polymeric materials, zeolite [15], chitosan [16], chitosan adipicate [17], phosphate cellulose [18], and carboneous particles [19] have also been tested as an anhydrous ER fluid particles. On the other hand, the continuous phases including silicone or hydrocarbon oils, possess low conductivity and large dielectric breakdown strength.

The well-known electrostatic polarization model incorporates the field-induced polarization of the dispersed phase particles relative to the continuous phase [20], in which the driving force of the particle fibrillation originates mainly from the electrostatic interaction among the particles. In addition, it plays a crucial role on the dielectric mismatch between the dispersed and the continuous phase which causes this interaction [21–23].

The PPP, which was one of the first reported particles to demonstrate blue electroluminescence, is a simple

conjugated polymer consisting of phenylene rings [24], and has recently been found to exhibit ER characteristics [25]. In this case, doping with FeCl_3 either in nitromethane solution [25] or aqueous solution [26] has played an important role in all of the previous studies on the PPP-based ER fluids. In contrast to this, the purpose of our study is to examine the ER response of PPP particles without doping. In general, most semi-conducting polymeric ER particles are treated via various dopants to enhance the conductivity of the particles. However, compared to these semi-conducting polymers, undoped PPP has also been found to show ER characteristics, even though the doping process influences the value of dielectric constant. Since the relevant physical process requires only a minor shift of the electric charges and thus it is more confined within a conjugated polymeric molecule, it seems to be less dependent on the sample structure than conductivity [27].

2. Experimental

The semi-conducting PPP is an insoluble, intractable, linear, rigid and infusible dark brown material with a low electric conductivity. The PPP particles were synthesized by adopting the procedure of Kovacic and Oziomek [28]. The detailed synthesis process and ER fluid preparation procedures were described in Sim *et al.* [29]. It has been also discovered that in most cases the synthesized PPP particles do not contain more than ten repeat units [30] because of the occurrence of side reactions, which destroy the functional groups and suppress the chain growth, and the occurrence of precipitating product from the solution [31].

The electrochemical polymerization of benzene has been typically performed under scrupulously anhydrous conditions in the media of low nucleophilicity and high activity. High activity reduces the oxidation potential of benzene and facilitates initiation of the polymerization by formation of σ - or π -complexes of benzene and a strong Lewis or Brønsted acid [32]. The kinematic viscosity and the density of the silicone oil were 30 cSt and 960 kg/m³, respectively.

Particle sizes and their distributions were measured by the particle size analyzer (Malvern MS 20, Malvern, UK) and particle shape was analyzed by scanning electron microscope (SEM S-2400, Hitachi, Hitachinaka, Japan). Density of the PPP particle was found to be 1210 kg/m³ by a pycnometer. The picoammeter (Keithley 487, Cleveland, USA) with custom-made cell (2 probes) was used to measure the conductivity of each sample pellet.

Electrorheological properties of the PPP-based ER fluids were measured using a rotational rheometer (Physica MC120, Stuttgart, Germany) with a Couette geometry equipped with a high-voltage generator (HVG 5000, Stuttgart, Germany). Temperature was controlled by a circulating oil bath. Several DC electric field strengths (1.0–3.5 kV/mm) were applied to the insulated bob. All measurement is conducted at 25°C, unless specified. The flow curves for each ER fluid were determined in the controlled shear rate mode, and the yield stress was then measured from controlled shear stress mode, which records the shear rate by presetting

the shear stress. The sample codes PPP-U3, PPP-U5, PPP-U7, and PPP-U10 represent 3, 5, 7, and 10 wt% of the undoped PPP in silicone oil, respectively. We also compared the ER characteristics of these undoped samples with 5 wt% FeCl_3 doped PPP ER fluids at two different particle concentrations (3 and 10 wt%). These two were denoted as PPP-3 and PPP-10, respectively. The PPP particle was doped with FeCl_3 in aqueous solution for 48 hours to increase conductivity following p-type (acceptor) doping method [27]. After doping, the PPP particles were then filtered and dried.

3. Results and discussion

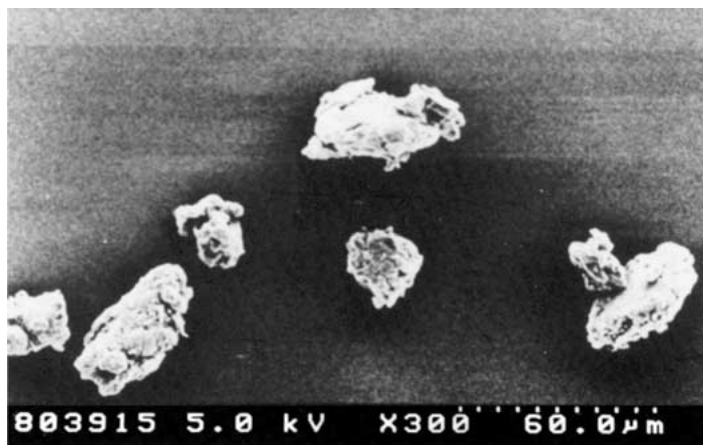
Fig. 1 shows the SEM photography of the PPP particles. The measured particle size distribution of the synthesized PPP was in the range of 15–25 μm (in diameter) and the shape was irregular for both the doped and the undoped PPP particles. The PPP based ER fluid is of technological interest, since the suspension microstructure and the particle interactions are sensitive to the change in rheological properties [33].

It is well known that charge injection onto conjugated, semiconducting macromolecular chains, “doping,” leads to the wide variety of interesting and important phenomena. Such polymers including polyaniline, polyacetylene and PPP can be made highly conductive in the presence of certain additives, called dopants. The reversible charge injection by doping can be accomplished in a number of ways, and the dopant may be electron acceptors such as arsenic pentafluoride and halogen, or electron dopants such as alkali metals.

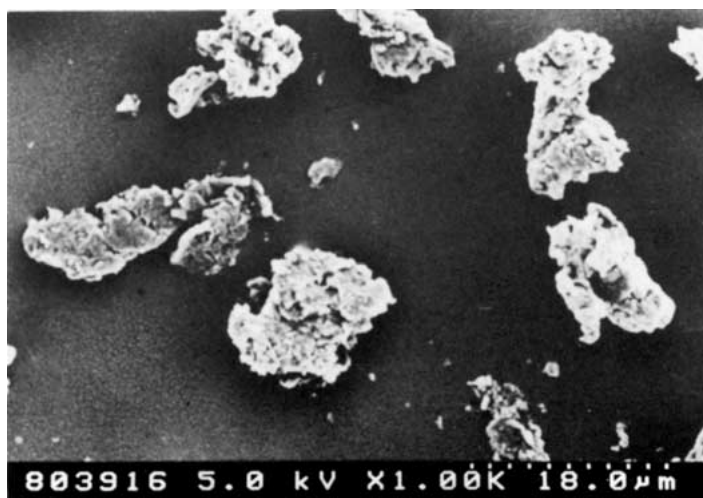
The conductivity varies with dopant concentration since doping may affect the charge rearrangement in polymer backbone [34]. The undoped PPP has conductivity of 1.12×10^{-13} S/m and 5 wt% FeCl_3 doped PPP has that of 4.40×10^{-10} S/cm. The conductivity determines the ER characteristics including the yield stress.

Figs 2 and 3 show the flow curves for shear stress and shear viscosity vs. shear rate of PPP-U7, respectively, at five different applied electric field strengths (0, 1.0, 2.0, 3.0, and 3.5 kV/mm). When an electric field is imposed, the rheological properties of an ER fluid vary by forming a fibrillated structure, with strings of particles oriented along the electric field direction. The shear stress initially decreased with shear rate, and then increased at the point of breaking as shown in Fig. 2. At the lower shear rate the fibrillated structure uniformly deformed first, a zone devoid of fibrils developed afterwards, and finally shearing from then on took place for the most part in the central region. Therefore, the largest increases in suspension viscosity occur at small shear rates and large field strengths [20].

The relative viscosity, which is scaled by that of the continuous phase, is plotted as a function of $\dot{\gamma}/E^2$ in Fig. 4. The data collapse onto a single curve. The value of suspension viscosity becomes larger as shear rates get smaller and/or electric field strengths become larger, as shown in Fig. 4. The drastic field-induced rheological property changes are accompanied by equally steep changes in the suspension microstructure. The particles rapidly aggregate into fibrous columns perpendicular to the electrodes.



(a)



(b)

Figure 1 SEM photography of (a) undoped PPP and (b) doped PPP.

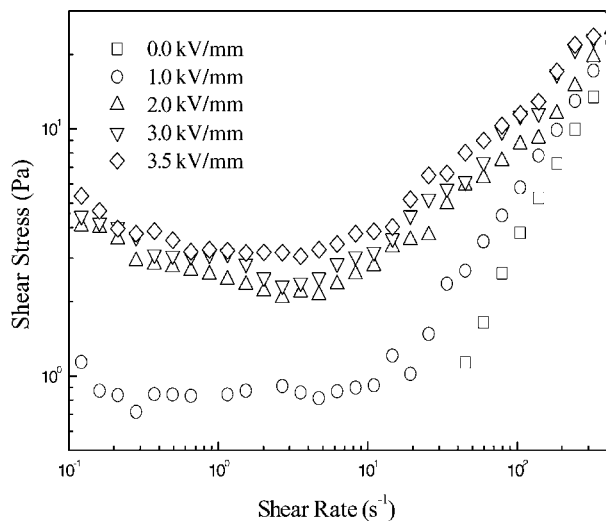


Figure 2 Shear stress vs. shear rate of PPP-U7 under various electric field strengths.

Fig. 5 shows measured shear stress for four different concentrations under the electric field strengths of 3.0 kV/mm. The shear stress increases with the PPP concentrations. In dilute suspensions, the electric field polarizes and aligns PPP particles, while the field-induced interactions result in the formation of particle chains at elevated electric field strengths. When the concentration gets larger than a few percent, particle

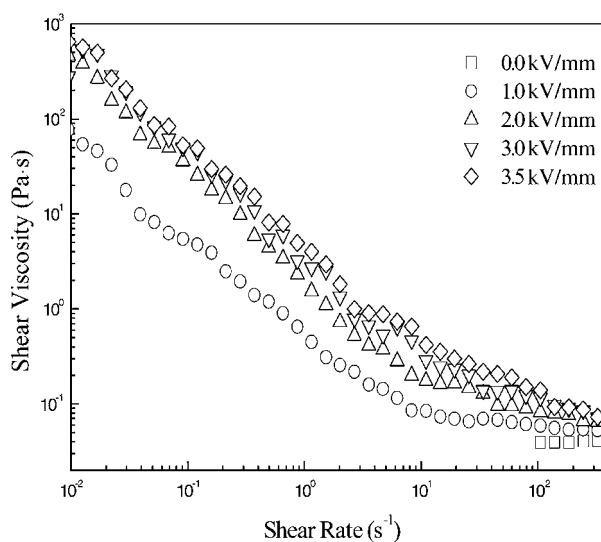


Figure 3 Shear viscosity vs. shear rate of PPP-U7 under various electric field strengths.

chains will percolate across the electrode gap and result in drastic changes in suspension rheology. Generally, the structure in a concentrated suspension can be sufficiently rigid to permit the material to withstand a certain level of deforming stress without flowing. The maximum stress that can be sustained without flow is called as “yield stress.”

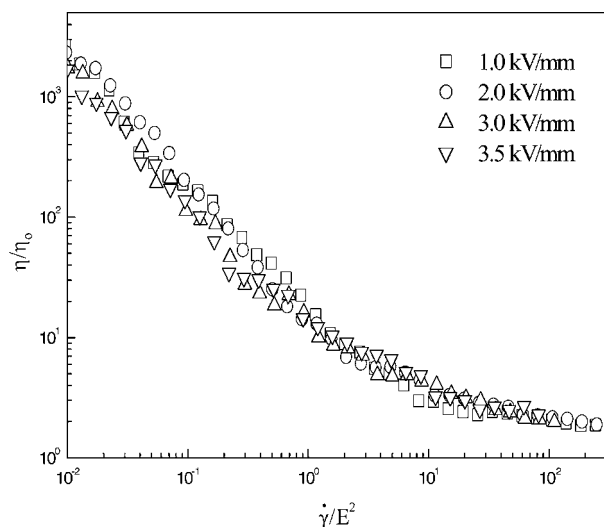


Figure 4 η/η_0 vs. $\dot{\gamma}/E^2$ of PPP-U7 under various electric field strengths. η_0 denotes the viscosity of the continuous phase.

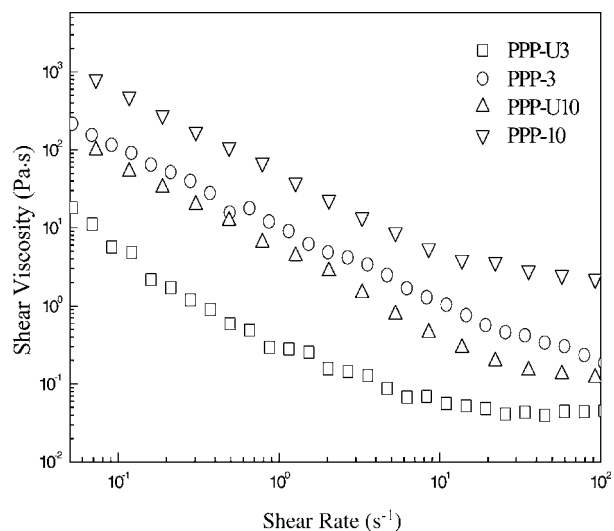


Figure 6 Shear viscosity vs. shear rate of PPP-U3, PPP-U10, PPP-3, and PPP-10 under the electric field strength of 3kV/mm.

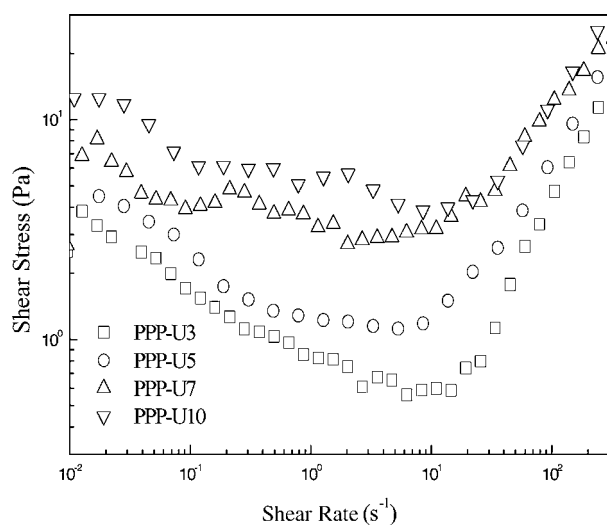


Figure 5 Shear stress vs. shear rate for PPP-U3, PPP-U5, PPP-U7, and PPP-U10 under the electric field strength of 3 kV/mm.

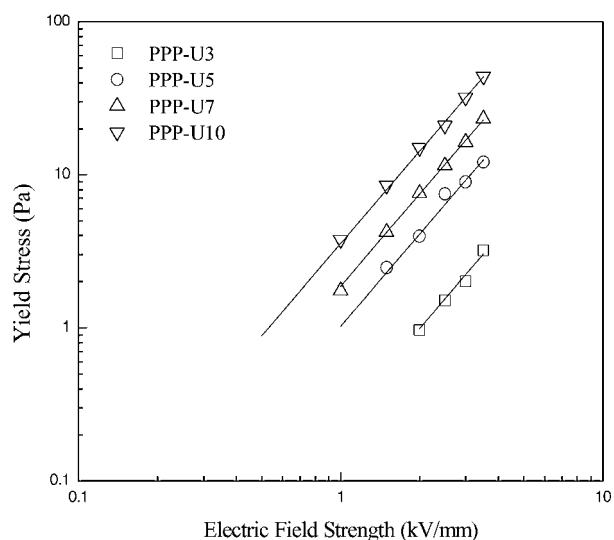


Figure 7 Yield stress vs. electric field strength for four different undoped PPPs.

Fig. 6 shows the flow curve of the PPP suspension for PPP-U3 & PPP-U10, and PPP-3 and PPP-10 respectively. The viscosities of the doped PPP suspension are higher than undoped PPP suspension under the electric field strength of 3 kV/mm. The PPP-3 has higher value than PPP-U10 even though the concentration of PPP-U10 is larger than that of PPP-3. This suggests that the undoped PPP particle suspension could also be used as a “model system” to test the doped system with low consideration by adopting the appropriate scaling theory described below.

Fig. 7 shows the yield stress for four different PPP concentrations with six different electric field strengths (E) (1.0, 1.5, 2.0, 2.5, 3.0, 3.5 kV/mm). The yield stress increases with concentration. The correlation between yield stress (τ_y) and electric field strength (E) for our system is presented as in power law form:

$$\tau_y(E) \propto E^m \quad (1)$$

The m values for the undoped PPP series were approximately 2. For the doped PPP, m approaches to 1.5 when E gets larger than 2 kV/mm [35].

To correlate yield stress in the broad range of electric field strengths, Choi *et al.* [36] introduced the following universal yield stress equation:

$$\tau_y(E) = \alpha E^2 \left(\frac{\tanh \sqrt{E/E_c}}{\sqrt{E/E_c}} \right) \quad (2)$$

Here, α depends on the dielectric constant and particle volume concentration and E_c is the critical electric field strength. For undoped PPP suspension, which is a special case of Equation 1, we conjectured that the E_c is much larger than our experimental E range, i.e., $E/E_c \ll 1$. In this limiting case, $\tanh(\sqrt{E/E_c}/\sqrt{E/E_c})$ approaches to unity, and Equation 2 reduces to power law.

$$\lim_{E/E_c \rightarrow 0} \tau_y(E) = \alpha E^2 \quad (3)$$

To obtain the the single scaling function for undoped PPP suspension, we scaled the yield stress values by choosing data for 2 kV/mm as a reference point, and

$$\tilde{\tau} = \tilde{E}^2 \quad (4)$$

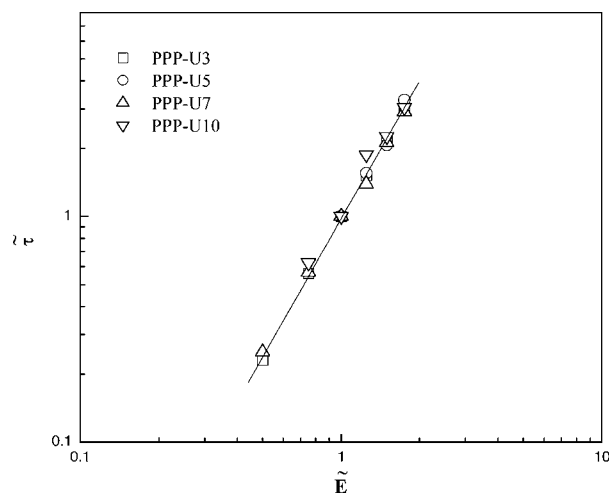


Figure 8 The scaling curve ($\tilde{\tau}$ vs. \tilde{E}) for four different undoped PPPs.

where $\tilde{E} \equiv E/(2 \text{ kV/mm})$ and $\tilde{\tau} \equiv \tau_y(E)/\tau_y(2 \text{ kV/mm})$. Our undoped PPP data are then collapsed onto a single curve using Equation 4, which is demonstrated in Fig. 8.

4. Conclusion

The suspension of undoped pristine PPP with four different weight concentrations in silicone oils exhibit the increase in the apparent shear viscosity under the given electric field strengths. Even though the ER properties of the undoped PPP are lower than those of the doped PPP, the shear stress and shear viscosity increase with electric field strength and weight concentration. The yield stresses of the undoped PPP based ER fluid increased with weight concentration, and were correlated very well with the universal scaling curve proposed by Choi *et al.* [36].

Acknowledgement

This research was supported by the Hallym Academy of Sciences at Hallym University, Korea, 2002-1.

References

1. R. TAO and J. M. SUN, *Phys. Rev. Lett.* **67** (1991) 398.
2. J. TRLICA, P. SÁHA, O. QUADRAT and J. STEJSKAL, *Physica A* **283** (2000) 337.
3. R. TAO, J. ZHANG, Y. SHIROYANAGI, X. TANG and X. ZHANG, *Inter. J. Mod. Phys. B* **15** (2001) 918.
4. Y. ZHANG, S. ZHANG and K. LU, *ibid.* **15** (2001) 596.
5. J. W. KIM, H. J. CHOI, H. G. LEE and S. B. CHOI, *J. Ind. Eng. Chem.* **7** (2001) 218.
6. S. G. KIM, J. W. KIM, M. S. CHO, H. J. CHOI and M. S. JHON, *J. Appl. Polym. Sci.* **79** (2001) 108.

7. J. H. LEE, M. S. CHO, H. J. CHOI and M. S. JHON, *Colloid. Polym. Sci.* **277** (1999) 73.
8. N. KURAMOTO, M. YAMAZAKI, K. NAGAI, K. KOYAMA, K. TANAKA, K. YATSUZUKA and Y. HIGASHIYAMA, *Rheol. Acta* **34** (1995) 298.
9. H. J. CHOI, J. W. KIM and K. TO, *Synth. Met.* **101** (1999) 697.
10. H. J. CHOI, M. S. CHO and M. S. JHON, *Inter. J. Modern. Phys. B* **13** (1999) 1901.
11. M. E. VASCHETTO, A. P. MONKMAN and M. SPRINGBORG, *J. Mol. Structure Theochem* **468** (1999) 181.
12. X. DUAN, W. LUO and W. WU, *J. Phys. D: Appl. Phys.* **33** (2000) 3102.
13. *Idem.*, *ibid.* **33** (2000) 696.
14. I. YANG and A. D. SHINE, *J. Rheol.* **36** (1992) 1079.
15. M. S. CHO, H. J. CHOI, I. J. CHIN and W. S. AHN, *Micropor. Mesopor. Mater.* **32** (1999) 233.
16. W. H. JANG, Y. H. CHO, J. W. KIM, H. J. CHOI, J. I. SHON and M. S. JHON, *J. Mater. Sci. Lett.* **20** (2001) 1029.
17. U. S. CHOI and Y. S. PARK, *J. Ind. Eng. Chem.* **7** (2001) 281.
18. S. G. KIM, H. J. CHOI and M. S. JHON, *Macromol. Chem. Phys.* **202** (2001) 521.
19. J. W. KIM, H. J. CHOI, S. H. YOON and M. S. JHON, *Inter. J. Mod. Phys. B* **15** (2001) 634.
20. M. PARTHASARATHY and D. J. KLINGENBERG, *Mat. Sci. Eng. R* **17** (1996) 57.
21. C. F. ZUKOSKI, *Ann. Rev. Mat. Sci.* **23** (1993) 45.
22. L. C. DAVIS, *J. Appl. Phys.* **72** (1992) 1334.
23. T. C. HALSEY, *Science* **258** (1992) 761.
24. G. GREM, G. LEDITZKY, B. ULLRICH and G. LEISING, *Adv. Mater.* **4** (1992) 36.
25. J. PLOCHARSKI, M. ROZANSKI and H. WYCISLIK, *Synth. Met.* **102** (1999) 1354.
26. H. J. CHOI, I. S. SIM and M. S. JHON, *J. Mater. Sci. Lett.* **19** (2000) 1629.
27. J. PLOCHARSKI, H. DRABIK, H. WYCISLIK and T. CIACH, *Synth. Met.* **88** (1997) 139.
28. P. KOVACIC and J. OZIOMEK, *J. Amer. Chem. Soc.* **85** (1962) 454.
29. I. S. SIM, J. W. KIM, H. J. CHOI, C. A. KIM and M. S. JHON, *Chem. Mater.* **13** (2001) 1243.
30. P. KOVACIC and M. B. JONES, *Chem. Rev.* **87** (1987) 357.
31. A. D. SCHLÜTER and G. WEGNER, *Acta. Polym.* **44** (1993) 59.
32. L. M. GOLDENBERG and P. C. LACAZE, *Synth. Met.* **58** (1993) 271.
33. W. B. RUSSEL, D. A. SARILLE and W. R. SCHOWALTER, "Colloidal Dispersions" (Cambridge University Press, Cambridge, 1989).
34. R. R. CHANCE, J. L. BRÉAS and R. SILBEY, *Phys. Rev. B* **29** (1984) 4491.
35. D. J. KLINGENBERG, F. VAN SWOL and C. F. ZUKOSKI, *J. Chem. Phys.* **94** (1991) 6170.
36. H. J. CHOI, M. S. CHO, J. W. KIM, C. A. KIM and M. S. JHON, *Appl. Phys. Lett.* **78** (2001) 3806.

Received 15 February
and accepted 6 May 2002